Chapter Two
An Overview of the Normal Stars

2.1 INTRODUCTION

Stellar spectra are astonishingly diverse. In the optical part of the spectrum, the vast majority are primarily absorption-line spectra, but even these range from the starkly simple A-type spectra, dominated by a few strong hydrogen lines, to the complex molecular spectra of M-type stars and carbon stars. For most stars, a solar mix of elemental abundances is a good first estimate, but there are some stars in which trace elements, such as the rare earths, or more common elements, such as carbon, are bizarrely enhanced. Some stars are hydrogen deficient, whereas others show marked underabundances of most metals. Certain stellar spectra, on the other hand, are dominated by emission lines. Wolf–Rayet stars, for example, show broad, strong emission lines in their spectra, clearly deriving from a massive stellar wind, whereas in the flare stars, common among the early M-type dwarfs, the emission lines are produced in active regions that might cover a significant fraction of the stellar surface.

This surprising diversity of spectral forms is a reflection of the wide range of physical phenomena that go into the formation of stellar spectra. It is remarkable, therefore, that the vast majority of stellar spectra can be comprehended on the basis of only two physical parameters—temperature and gas pressure (or its proxies, surface gravity and density). The purpose of this chapter is to take a first look at the variety of stellar types explained by those two physical parameters. First, we survey the two-dimensional array of *normal* stellar types from a descriptive, morphological point of view (the basis of the MK spectral classification system); second, we briefly examine an independent technique for classifying stars, i.e., multicolor photometry; and then, finally, we explore, using simple concepts from physics, how those two physical parameters can account for the observed array of spectral forms of normal stars.

2.2 THE SPECTRAL SEQUENCE

2.2.1 The Main Sequence

In Chapter 1 we traced the history of the MK spectral classification system, including the realization that the sequence of spectral types OBAFGKM represents a temperature sequence. That this ordering of spectral types is a temperature sequence is abundantly clear from Figure 2.1, which shows how the optical spectral

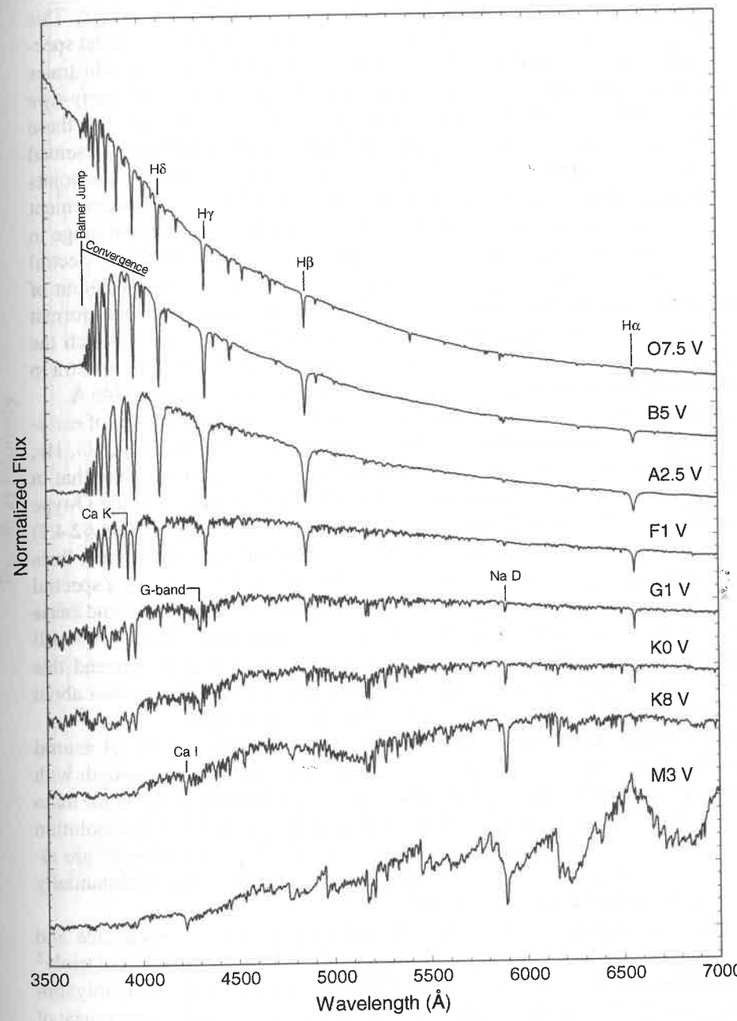

Figure 2.1 The OBAFGKM spectral sequence for main-sequence (dwarf) stars illustrating that the spectral sequence is ordered in terms of temperature. Here, the normalized stellar flux (the *energy distribution*) is plotted against wavelength. Some of the more prominent spectral features are marked, including the Balmer jump and convergence. The source of these spectra is the Indo-US coudé-feed spectral library (Valdes et al. 2004). The spectra have been normalized at a common wavelength, and separated by one continuum unit for clarity, except for the bottom spectrum, which is offset by 2 units.

energy distributions of main-sequence (*dwarf*[1]) stars vary with spectral type. This sequence is presented in more detail in Figures 2.2 and 2.3 in the blue-violet spectral region traditionally used for MK spectral classification. Figure 2.2 illustrates stars hotter than the Sun (these stars are commonly referred to as the *early-type stars*), and Figure 2.3 stars cooler than the Sun, the *late-type stars*. Note that these figures use two different spectral formats. In Figure 2.2 the spectra are presented in "rectified" format, in which the intensity of the continuum points (i.e., the points not affected by line absorption) has been normalized to unity. This is a convenient format to use as it permits the use of line ratios over a wide wavelength range in spectral classification. However, in the late-type stars, the density of the spectral lines is so great that there are no true continuum points, and so rectification of the spectrum is not the best representation. Instead, the most convenient format for these spectra in classification is the "normalized flux" format, in which the stellar fluxes have been normalized to unity at one common point. The spectra in Figure 2.3 have been normalized to unity at a common wavelength of 5445 Å.

A glance at Figure 2.2 indicates that the salient feature of the sequence of early-type spectra is the behavior of the hydrogen Balmer lines (the Hβ, Hγ, Hδ, Hϵ, H8, and H9 lines in the Balmer series are visible in these spectra). Note that in the O-type stars, the hottest normal stars, the Balmer lines (which in the O-type stars are actually blended with lines of the Pickering series of He II—see §2.4.2) are quite weak. With decreasing temperature (later spectral type), the Balmer lines increase in strength, coming to a maximum in the early A-type stars, at a spectral type of about A2. They then fade rapidly with decreasing temperature, and cease to dominate the blue-violet spectrum in K-type and later stars. In §2.4 we will use elementary concepts from atomic and statistical physics to understand this behavior. For the moment, it is sufficient to note that this behavior comes about through the interplay of the ionization and excitation of hydrogen.

Lines of other species show a similar behavior. For instance, lines of neutral helium (He I) are very weak in the early O-type stars, but grow in strength with decreasing temperature, coming to a maximum at a spectral type of B2 on the main sequence. They then fade and essentially disappear from classification–resolution spectra by A0. In the O-type stars, lines of singly ionized helium (He II) are already declining in strength; their peak would be attained only in stars substantially hotter than the hottest known O-type star.

Another outstanding feature of the spectral sequence is the appearance and rapidly growing strength of lines due to metals. While lines of doubly and triply[2] ionized metals appear in the spectra of the O-type stars, and singly and doubly ionized metals in the B-type stars, lines of metals begin to dominate the appearance of the blue-violet spectrum only in the A-type stars. The strongest metal line in this

[1]The terms *dwarf*, *giant*, and *supergiant* are commonly used to refer to stars that inhabit different parts of the *Hertzsprung–Russell diagram* (see Glossary). Stars on the main sequence are called dwarfs, whereas giants and supergiants have evolved off the main sequence.

[2]Notation such as Fe I, Fe II, Fe III, etc. is used to represent different ionization states of an atomic species. Thus, Fe I refers to neutral iron, Fe II to singly ionized iron (Fe^{+1}), Fe III to doubly ionized iron, etc.

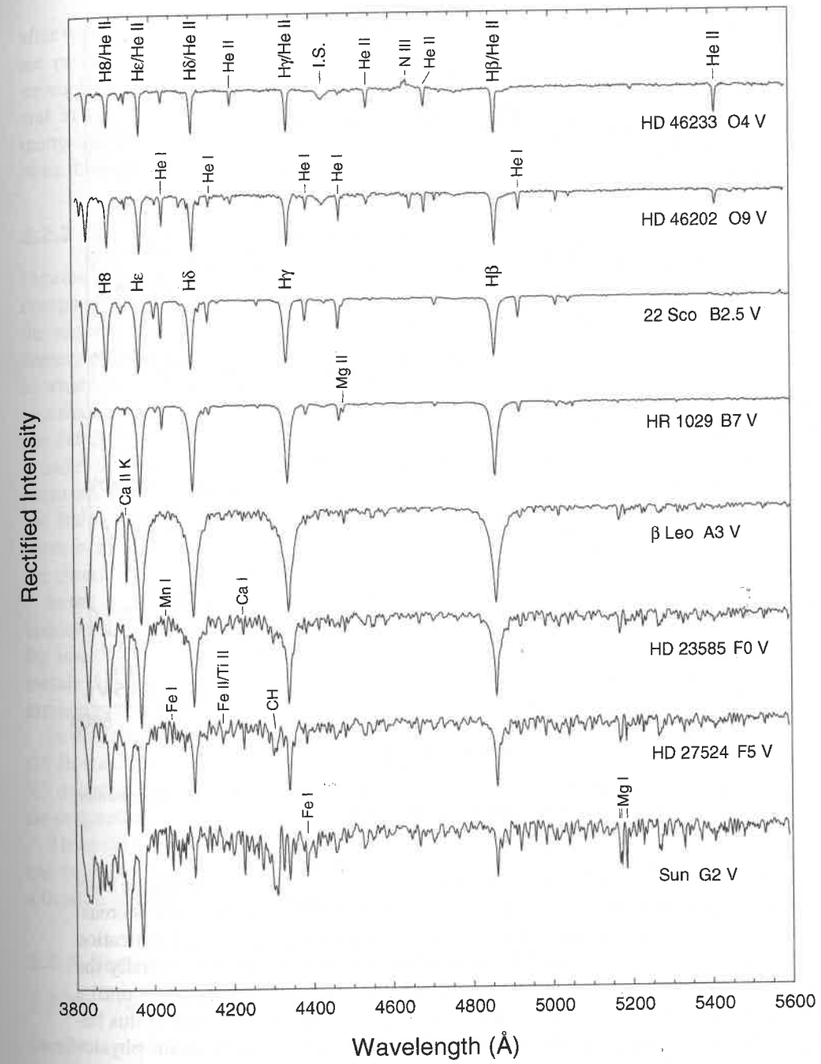

Figure 2.2 The Main Sequence from O4 to G2. Spectra in Figures 2.2–2.5 were obtained with the GM spectrograph on the 32″ telescope of the Dark Sky Observatory. These rectified spectra have a resolution of 3.6 Å, and have been offset by 0.7 continuum units for clarity.

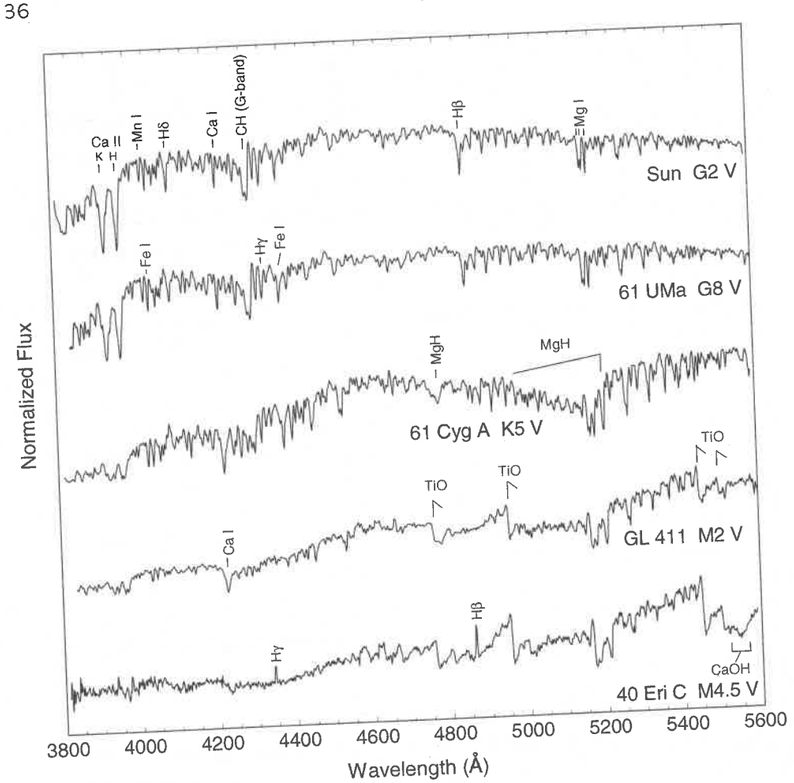

Figure 2.3 The Main Sequence from G2 to M4.5. These flux-calibrated spectra have been normalized at 5445 Å, and given integer vertical offsets for clarity.

spectral region, the Ca II K-line, first appears at a spectral type of B9 (some stars of earlier types show an interstellar Ca II K-line), and grows rapidly with decreasing temperature. Some of the metal lines commonly used in spectral classification are marked in Figures 2.2 and 2.3. Notice that most of these lines, especially the lines due to neutral species, grow in strength with decreasing temperature until a spectral type of K5, after which many begin to decline in strength. While this behavior appears superficially like that of the hydrogen and helium lines, the physics governing these line strengths is considerably more complex. We will consider this physics in more detail in §2.4.

Finally, spectral features due to molecules make their first appearance in the early F-type stars. The feature marked "CH" in the F5 star in Figure 2.2 is due to the diatomic molecule CH and is called the G-band. This molecular band grows rapidly in strength and comes to a maximum in the dwarfs at a spectral type of K2,

after which it fades away. In the K-type stars, molecular bands due to CN and MgH are prominent in the blue-violet region. The M-type spectra are dominated by strong bands of TiO. In even later spectra (as we will see in Chapters 8, 9 and 10), and in spectra of stars with unusual abundances (see, for instance, Chapter 8), many other molecules make their appearance, including polyatomic molecules. Note the band due to CaOH in the M4.5 dwarf in Figure 2.3.

2.2.2 Supergiants

Figures 2.4 and 2.5 present similar sequences for Ib supergiant stars and can be compared directly with Figures 2.2 and 2.3 for the dwarfs. Note that superficially the sequences appear very similar. However, there are a number of important differences. Consider the Balmer lines. In the supergiants, we see a behavior similar to what we saw in the dwarfs; the Balmer lines are weak in the O-type stars, come to a maximum in the A-type stars, and then fade for later spectral types. However, the details are different. Notice that for the early-type stars the Balmer lines are broader in the dwarfs than in the supergiants, and that in the supergiants the maximum occurs at a later spectral type. For instance, in the dwarfs the maximum in the Balmer lines occurs at a spectral type of A2; in the Ib supergiants the maximum is in the late A-type stars, or even at F0. Later than F0 the Balmer lines in the dwarfs and supergiants have essentially the same strengths.

In the A-, F-, and G-type supergiants, the metal lines are, with few exceptions, considerably stronger than the same lines in the dwarfs. This is particularly true for lines of ionized metals; some prominent lines and blends of lines of ionized metals that have significantly different strengths in the dwarfs and supergiants are marked in Figure 2.4.

In the late-type supergiants (Figure 2.5) note the strong CN band in 9 Peg, the G5 Ib standard, and its absence in the G-dwarfs (Figure 2.3). In addition, in the K5 dwarf in Figure 2.3, two molecular bands due to MgH are prominent, whereas these spectral features are weak or absent in the supergiants.

These differences (and others) in the spectra of main-sequence and evolved stars can be exploited in *luminosity classification*. A brief overview of luminosity classification is given in §2.2.4, but the details are best left for later chapters.

2.2.3 Sequences in the Ultraviolet and Infrared

2.2.3.1 The Ultraviolet

Ideally, a star should be classified in the region of the spectrum where its energy distribution peaks. Thus, the hot O- and B-type stars are ideally classified in the ultraviolet, A- through K-type stars in the optical, and M-type and later objects in the red and infrared. Of course, for ground-based telescopes, the ultraviolet and much of the infrared are inaccessible, a fact that in the past dictated that spectral classification was carried out largely in the optical. Other considerations may also require that stars be classified in spectral regions far from their flux peak. For instance,

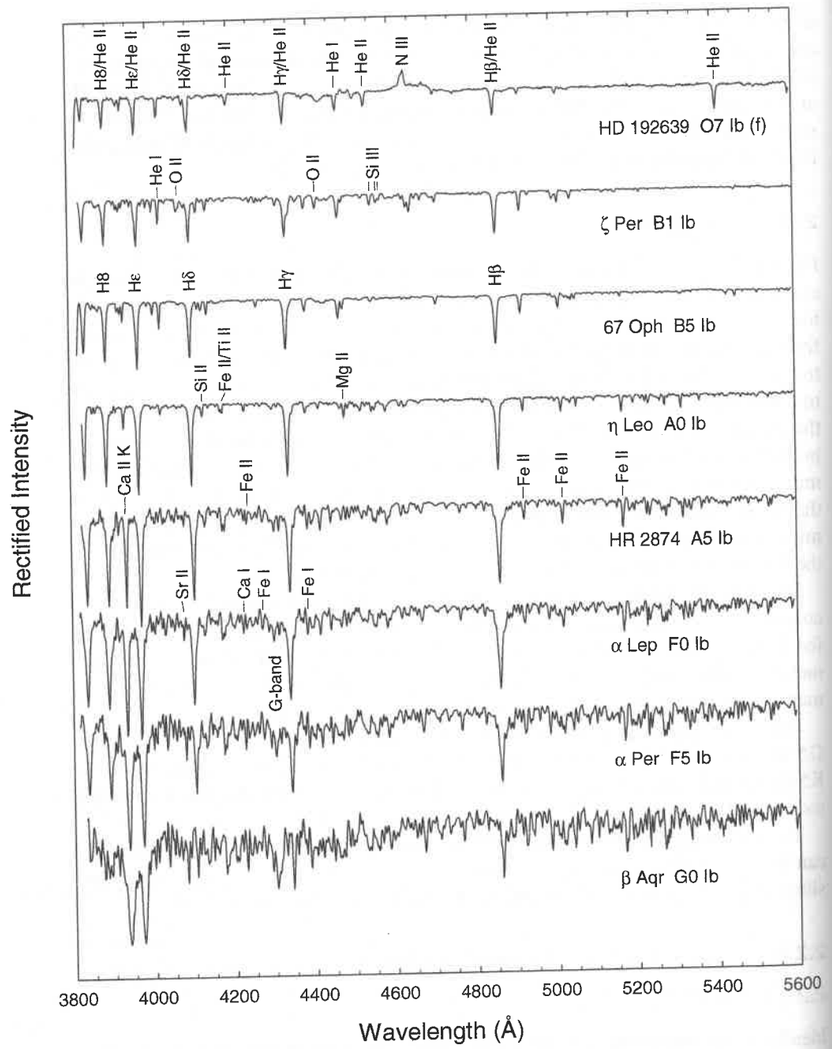

Figure 2.4 Ib Supergiants from O7 to G0. These spectra are rectified, and have been offset vertically by 0.7 continuum units.

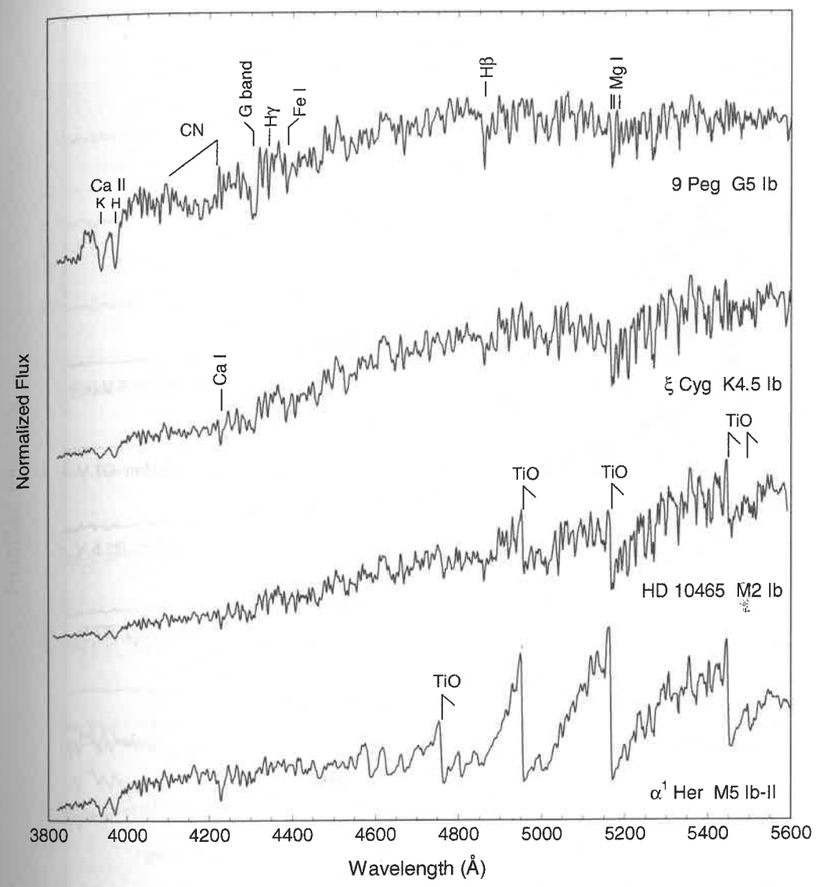

Figure 2.5 Ib Supergiants from G5 to M5. These spectra are in normalized flux format, and have been given integer vertical offsets for clarity.

in star-formation regions, the presence of dust may cause such large extinctions in the ultraviolet and optical that observations in those spectral regions are impossible. In such circumstances, observing and classifying O- and B-type stars in the infrared may be the only option. We will consider one such classification system for the O- and B-type stars in Chapter 3.

Figures 2.6 and 2.7 show spectral sequences for main-sequence stars in the ultraviolet and in the H-band region ($\approx$1.65 μm) of the infrared. The ultraviolet montage is based on spectra obtained with the International Ultraviolet Explorer

spacecraft (IUE) in the low dispersion mode. The infrared sequence is based on spectra obtained by Meyer et al. (1998). In the ultraviolet sequence, we have displayed the spectra in the normalized flux format to illustrate the enormous change in the ultraviolet flux as the temperature decreases. For stars much cooler than the Sun, the photospheric contribution to the ultraviolet region is minimal and instead this region is dominated by chromospheric and coronal emission lines. The strengths of these emission lines depend strongly on factors other than temperature and gravity (for instance, rotation and magnetic field strength), and thus cannot be used in a spectral classification system organized according to temperature and luminosity.

In Chapters 3 and 4 we will consider spectral classification systems for the O- and B-type stars based on high-resolution ultraviolet spectra. Figure 2.6 uses low-resolution IUE spectra, with a resolution of only about 6–9 Å. Even at such a low resolution features useful for spectral classification are visible. Notice in the O3.5 V spectrum the presence of strong lines due to highly ionized species (N V, Fe V, O V, C IV). The C IV feature exhibits a P Cygni profile consisting of a strong, blue-shifted absorption component combined with an emission component. This profile is the signature of a stellar wind; the absorption component is formed in the cylinder of expanding gas that we see in front of the stellar disk and the emission component from the remainder of the expanding shell (see Figure G.2). A similar profile can be seen for the N V line. While nearly all classes of stars have stellar winds, the mass-loss rates decline precipitously along the main sequence, and thus spectral wind features tend to fade toward later types.

The strongest line in the B-type stars in the ultraviolet region is the hydrogen Lyman-α line (1216 Å). Other lines in the Lyman series lie outside of the IUE spectral range but have been observed with the FUSE satellite (see Chapters 3 and 11). It is of interest to note that no lines of He I appear in the IUE spectral range. Lines of ionized helium do appear in this region, but are generally weak and not easily discerned at low resolution.

As we proceed toward cooler types in Figure 2.6, the flux in the far (shortwave) ultraviolet becomes less dominant, and the species that form the strongest lines tend to be in lower ionization states. In the A- and F-type stars, the shortwave ultraviolet vanishes. This is partly a consequence of the cooler temperatures of these stars, but also caused by the presence of both strong continuous and line absorption due to metals (see §2.4) in the atmospheres of these stars. A prominent feature that grows rapidly with declining temperature in the A- and F-type stars is the Mg II line (actually a blend of two strong lines, the Mg II h and k lines). These lines arise from energy levels analogous to those in the Ca II ion that give rise to the Ca II H and K lines and thus behave in a similar way.

2.2.3.2 The Infrared

The infrared is traditionally divided into a number spectral regions accessible from the ground through atmospheric "windows." The regions or "bands" most often

utilized for stellar spectroscopy include the J-band ($\approx$1.24 μm), the H-band ($\approx$1.65 μm), the K-band ($\approx$2.2 μm) and the L-band ($\approx$3.4 μm). Other regions in the infrared tend to have too much telluric (terrestrial atmospheric) absorption to make ground-based spectroscopy practical, and thus can be exploited only by space-based instruments (see §13.3).

For pedagogical purposes we will confine our discussion of the infrared in this chapter to the H-band sequence of main-sequence stars presented in Figure 2.7. Detailed spectral sequences in the J-, H-, K-, and L-bands for the different spectral types will be presented in later chapters.

The spectra of early-type stars in the H-band are dominated by lines of hydrogen. In the H-band, these hydrogen lines are members of the Brackett series (which arise from transitions out of the $n=4$ energy level; the Balmer series, which is visible in the optical and near ultraviolet, arises from transitions out the $n=2$ energy level in the hydrogen atom). Only the higher lines in the Brackett series are visible here; Brackett-α lies at about 4 μm and Brackett-γ is in the K-band. The designation we will use in this book for hydrogen (and He II) lines higher than ϵ in a series is the principal quantum number of the upper energy level of the transition. Thus, Balmer H8 arises from the transition $2 \rightarrow 8$, Brackett-10 from the transition $4 \rightarrow 10$.

The behavior of these hydrogen lines is quite similar to that of the Balmer lines in the optical; the hydrogen lines are relatively weak in the hottest stars, come to a maximum at an intermediate temperature, and then fade in the F- and G-type stars. A comparison with Figure 2.2, however, shows a subtle difference. In the optical, the hydrogen lines come to a maximum at A2 in the dwarf stars. In the H-band we see that B7 and A3 stars have hydrogen-line strengths that are nearly identical, implying that the maximum lies closer to A0, and may even be in the late B-type dwarfs. This difference is easily understood on the basis that the Brackett lines arise from a higher level in the hydrogen atom than the Balmer lines, as we will see in §2.4.

Other features show behaviors similar to the optical. Lines due to neutral metals gradually strengthen as we go toward later types, and come to a maximum at a spectral type of about K7, after which they tend to fade. Molecular absorption is less important in the H-band than in the optical, however. The prominent TiO bands that dominate the spectra of M-dwarfs in the optical extend only to about 1 μm, and thus do not contribute to the H-band. The only molecules that show absorption features strong enough to be easily visible in these H-band spectra are CO and OH.

2.2.4 Luminosity Classification

The MK System is fundamentally a two-dimensional system, consisting of a temperature dimension (*the spectral sequence*), which we considered in outline in the previous sections, and a luminosity dimension, which separates dwarfs (main-sequence stars) from evolved stars. Table 2.1 lists the main luminosity classes

Table 2.1 Luminosity Class (L.C.) Notation

L.C.	Name	L.C.	name
V	dwarf	Ib	supergiant
IV	subgiant	Ia	bright supergiant
III	giant	0	hypergiant
II	bright giant		

employed in the MK System, but be aware that subdivisions (such as IV–V) are commonly employed, and that the notation for these subdivisions can vary from one spectral class to the next, mostly for historical reasons. The luminosity class VI has been used historically to classify stars that lie below the main sequence in luminosity (i.e., the so-called *subdwarfs*) but this notation is no longer commonly employed (for exceptions see Chapters 4, 9, and 10).

Luminosity classification is carried out using spectral criteria that are peculiar to the spectral class, and even, in some cases, spectral subclass, and thus the details of luminosity classification are best left to the later chapters that are devoted to the individual spectral classes.

However, to establish some terminology, let us consider two specific examples. If a spectral feature strengthens with increasing luminosity (i.e., if it strengthens along the sequence V → III → I), then we say that it exhibits a *positive luminosity effect*. On the other hand, if it weakens along the same sequence, we say that it exhibits a *negative luminosity effect*. The hydrogen lines in the early A-type stars exhibit a negative luminosity effect. Compare the width of the hydrogen lines in the A3 V star in Figure 2.2 with the hydrogen lines of the supergiant A0 and A5 stars in Figure 2.4. The marked narrowing of the hydrogen lines with increasing luminosity in the early A-type stars can be used as a sensitive luminosity criterion. On the other hand, lines of Fe II and Ti II in the F-type stars tend to increase in strength with increasing luminosity. For instance, compare the Fe II/Ti II feature at λλ4172–8 marked in the dwarf sequence in Figure 2.2 with the same feature in the supergiants in Figure 2.4. This is an example of a luminosity criterion that exhibits a positive luminosity effect.

2.3 MULTICOLOR PHOTOMETRY AND STELLAR CLASSIFICATION

In the previous section, we reviewed the outline of stellar spectral classification. The rest of the book will fill in the details! It should be noted at this point, however, that stellar classification may be carried out using techniques other than spectroscopy. In particular, stars may be classified, or at least characterized, with multicolor photometry. There are many existing systems of multicolor photometry, but all have in common the use of measurements of stellar brightnesses or *fluxes* in certain spectral bands. The isolation of the stellar bands is usually accomplished with glass and/or interference filters, and the flux measurements, traditionally obtained with photomultipliers, are now increasingly being acquired with CCDs.

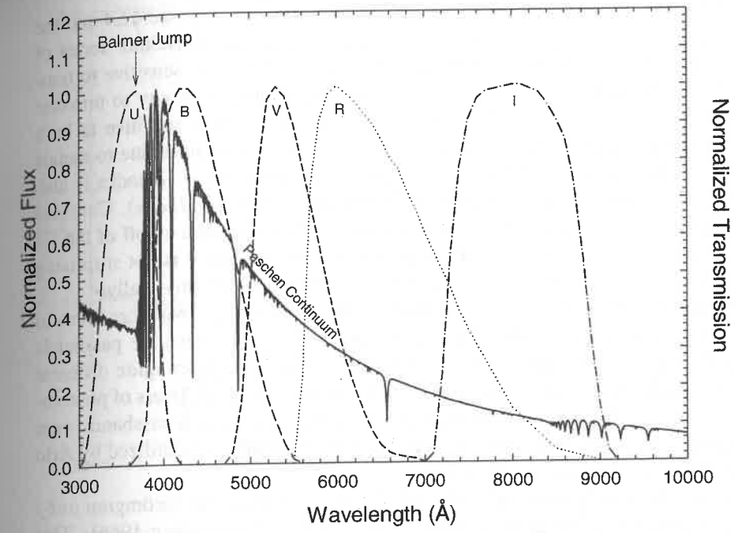

Figure 2.8 The normalized Johnson–Cousins *UBVRI* photometric passbands (right-hand scale) plotted with the spectral energy distribution of an A0 V star (left-hand scale). The stellar energy distribution has been normalized to unity at the highest point. Notice the positions of the Balmer jump and the Paschen continuum. The Balmer lines are easily visible, and converge at a wavelength of 3646 Å. The scale of the right-hand vertical axis is identical to the left.

Multicolor photometry has a long and interesting history, but even a precis of that history is beyond the scope of this book. Interested readers are referred to the book *The Measurement of Starlight: Two Centuries of Astronomical Photometry* by Hearnshaw (2005). In the modern era, the most widely used, although not necessarily the best designed, photometric system is the Johnson *UBV* system (Johnson & Morgan 1953). Figure 2.8 shows the stellar energy distribution (flux spectrum) of an A0 V star plotted with the transmission passbands of the *U* (ultraviolet), *B* (blue), and *V* ("visual" or yellow-green) filters. In normal practice, stellar fluxes measured through these filters are converted to magnitudes, and placed on the standard *UBV* system via observations of standard stars. These magnitudes may be used to form the *photometric indices* $U-B$ and $B-V$. The $B-V$ index (or color) is a measure of the slope of the Paschen continuum (see Figure 2.8), and as such is quite closely correlated with the *effective temperature* of the star, although dwarfs and giants must be considered separately, and metal-weak stars do not obey the same relation as metal-rich. The $U-B$ index is also related to temperature, and is especially useful in the early-type stars for that purpose, but it is sensitive to other factors as well. Figure 2.8 shows that the *U* and *B* filters span and overlap the *Balmer jump*, a spectral discontinuity caused by the

photoionization of hydrogen from the first excited level ($n = 2$; see §2.4 and the discussion of *continuous opacity*), and the convergence of the Balmer series of hydrogen lines. The "height" of the Balmer jump is primarily sensitive to temperature in the early-type stars, but also shows significant sensitivity to pressure (surface gravity) in the A- and F-type stars, and thus $U{-}B$ is sensitive to both temperature and gravity. But, because the density of spectral lines due to metals is greater shortwards of the Balmer jump than longwards, the $U{-}B$ index is also sensitive to the overall metal abundance (sometimes called *metallicity*). Combine these various sensitivities with the fact that the short-wavelength cutoff of the U-filter passband is actually set by atmospheric absorption, and it is not surprising that the $U{-}B$ index can be difficult to interpret and model astrophysically.

UBV photometry is quite often combined with photometry in two other filters in the red and near-infrared, the R and I filters. Figure 2.8 shows the passbands of the R and I filters on the Johnson–Cousins system, which are quite different from the passbands of the R and I filters on the Johnson system. Users of photometry published in the literature must be careful to ascertain which passbands were employed. The Johnson–Cousins system has been carefully standardized by Arlo Landolt (see, for instance, Landolt 1992).

Another commonly used multicolor photometric system is the Strömgren *uvby* system, designed by Bengt Strömgren in the 1960s (see Strömgren 1966). This system employs filters with narrower passbands than the Johnson *UBV* system; this enables the color indices on this system to be more easily interpreted astrophysically. Figure 2.9 plots the passbands of the four Strömgren filters with the energy distribution of an A0 V star. Notice that the u (ultraviolet) and v (violet) filters are more intelligently placed with respect to the Balmer jump and convergence than in the *UBV* system, although the Hδ line lies within the passband of the v filter. The $b{-}y$ index measures, like the $B{-}V$ index on the Johnson system, the slope of the Paschen continuum. Two other indices are defined in the Strömgren system. The m_1 index, defined by $m_1 = (v{-}b) - (b{-}y)$, was designed to measure the *line blanketing* (absorption by spectral lines) in the v band; the $(b{-}y)$ term in the definition of the m_1 index helps to remove, to first order, the temperature sensitivity of this index. The c_1 index, defined by $c_1 = (u{-}v) - (v{-}b)$, measures the height of the Balmer jump, and is relatively free of the photometric effects of the Balmer convergence, unlike the $U{-}B$ index. In addition, the $(v{-}b)$ term in the definition of the c_1 index removes, to first order, the metallicity sensitivity of that index. The c_1 index comes to a maximum in the early A-type stars, like the hydrogen Balmer lines (see §2.2 and Figure 2.10). Strömgren photometry was designed explicitly for the detection and study of metal-weak F- and G-type stars, but has also found applications in the B-, A-, K-, and M-type stars (see, for instance Crawford 1975, 1978, 1979; Olsen 1983; Olsen & Perry 1984; Olsen 1995).

Strömgren *uvby* photometry is often used with Hβ photometry, which consists of two filters centered on the hydrogen (Balmer) β line. One filter is narrow (full-width $\approx$60 Å), the other is wider (full-width $\approx$300 Å; see Crawford & Mander 1966). The inclusion of Hβ photometry helps in the determination of interstellar reddening.

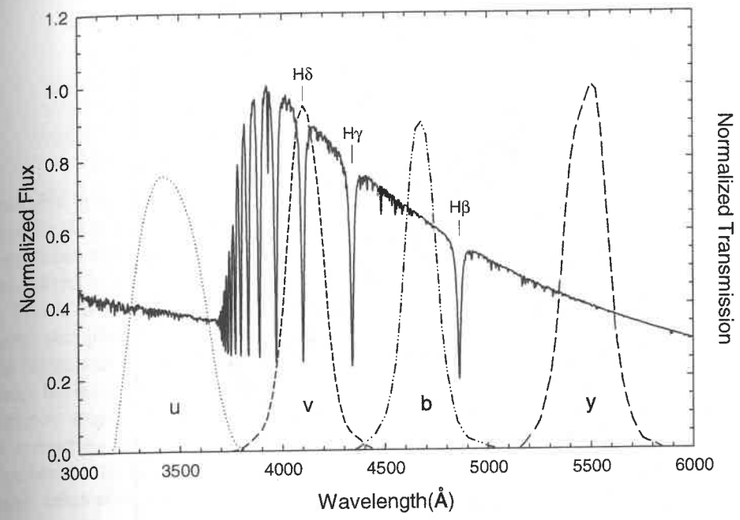

Figure 2.9 The Strömgren *uvby* photometric passbands (right) plotted with the spectral energy distribution of an A0 V star (left). Notice that the narrower bands of the Strömgren system more cleanly sample the Balmer jump than the Johnson *UBV* passbands. The Strömgren passbands in this figure have been normalized to the peak transmission of the y band. The scales of the two vertical axes are identical.

A more recent photometric system, combining some of the filter passbands of the Strömgren system with those of the Vilnius system, has been developed, largely through the efforts of Straižys and colleagues (Straižys et al. 1996). This new system is called Strömvil photometry, and time will tell whether it will be widely adopted. Another photometric system that has similar properties to the Strömgren system is Geneva photometry (see, for instance, Nicolet 1996).

Yet another recently developed photometric system is the $u'g'r'i'z'$ Sloan Digital Sky Survey (SDSS) photometric system. The sixth release of data from the SDSS contains photometry of 287 million unique objects, including stars and galaxies. Table 2.2 lists the effective wavelengths of the five Sloan filters. For more information on the survey and $u'g'r'i'z'$ photometry, see `http://www.sdss.org`.

Over the years a large number of photometric systems have been developed, often for special purposes. It is beyond the scope of this book to review these systems, but the following merit mention: the DDO system for the measurement of red giants, incorporating filters to sample the CN molecular bands (McClure 1976); the Wing narrow-band system for late-type stars (White & Wing 1978); and the Washington system for late-type stars (Canterna 1976). Photometric systems have also been defined for the ultraviolet and infrared, such as the 2MASS JHK infrared photometric system (Skrutskie et al. 2006).

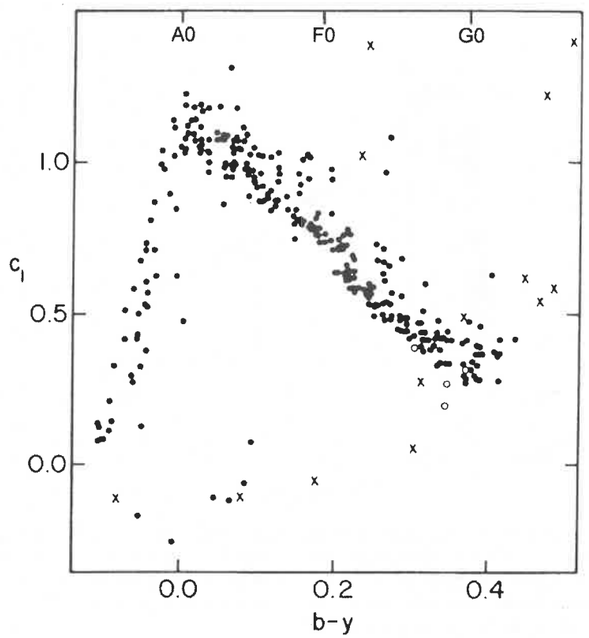

Figure 2.10 The $b-y$ index plotted against the c_1 index for the bright stars. Both indices are on the Strömgren $uvby$ photometric system. The $b-y$ index, in the absence of reddening, measures the temperature, the c_1 index, the Balmer jump. Note that the c_1 index comes to a maximum near $b-y = 0.0$, corresponding to the early A-type stars. The approximate positions of main-sequence spectral types have been added to the top scale for reference purposes. Figure from Crawford (1984) and used with permission from the David Dunlap Observatory.

Every photometric system can be calibrated against MK spectral types; for instance, by observing a large number of A0 V stars, it is possible to find mean $b-y$, m_1, and c_1 indices for that spectral type. Tabulations of such mean values can be found in a number of sources, including Drilling & Landolt (1999). Some astronomers have been tempted to reverse the process, i.e., to obtain photometric indices for their stars of interest, and then to "derive" MK spectral types via the tabulations. This practice is deprecated (see, for instance, the comments after the paper by Heck 1984), as an MK type is properly determined only through detailed comparison of the unknown spectrum with the MK standards. As will become evident in the following chapters, the combined effects of rotation, metallicity, interstellar reddening, and other *photometric degeneracies* can confuse the translation of photometric indices into MK types, even if such a translation were

Table 2.2 SDSS filter Effective Wavelengths

u'	g'	r'	i'	z'
3551 Å	4686 Å	6165 Å	7481 Å	8931 Å

desirable or legitimate. Rather, the MK type should be regarded as an independent datum of stellar astronomy, capable of yielding insight and information when confronted with other data types, such as photometry. Some of these issues are considered in more detail by Crawford (1984) and Gray (2006).

That is to say, the most productive relationship between MK classification and multicolor photometry is one of *complementarity*. The complementary nature of the interaction between spectral classification and multicolor photometry comes about because these two systems approach the classification of stars in two very different ways. Multicolor photometric systems, for the most part, are confined to measuring continuum features in a stellar spectrum, such as the slope of the Paschen continuum, the Balmer jump, etc. Spectral classification, on the other hand, relies almost entirely on the appearance of the line spectrum. In most cases, the two systems give consistent classifications, but the most interesting comparisons arise when the two systems *disagree*. In that disagreement is often found new information about stellar atmospheres, stellar evolution, or even the interstellar medium. Thus, one's spectral type for a given star should never be influenced by photometric information, because that influence would rob the interface between the two systems of any information content.

The first, and in some ways still the best, example of complementarity between the two systems is the determination of reddening due to the presence of interstellar dust. Interstellar dust *reddens* the light from a star by preferentially scattering out of the line of sight short wavelength light. Reddening, of course, affects the photometric measurement of the color of the star (for instance, the B–V and $b-y$ indices are made more positive), but has little effect on the line spectrum and thus the spectral type. Therefore, if *intrinsic colors* for the different spectral types are found by studying nearby, unreddened stars, the *color excess*, or *reddening*, for a given star may be determined by comparing the measured color index to the intrinsic color index determined from its spectral type. These color excesses take the form

$$E(B-V) = (B-V) - (B-V)_0 \tag{2.3.1}$$

where $(B$–$V)_0$ is the intrinsic color of the star.

There are many other instances of complementarity between photometry and spectral classification; the history of the Strömgren $uvby\beta$ system is particularly rich in examples. This profitable interaction has been expertly reviewed by Olsen (1994).

2.4 PHYSICAL PRINCIPLES UNDERLYING THE MK SEQUENCE

2.4.1 Physical Conditions in Stellar Photospheres

While a theoretical understanding of the formation of the stellar spectrum is certainly not necessary for the process of spectral classification, it is essential for the *interpretation* of spectral types. It is beyond the scope of this book to develop the theory of stellar atmospheres and spectral-line formation in detail; excellent monographs exist on that subject (i.e., *The Observation and Analysis of Stellar Photospheres*, Gray 2008; and *Stellar Atmospheres*, Mihalas 1978). However, it is possible to gain a physical understanding of the spectral sequence and other aspects of stellar spectral classification by considering some elementary results of statistical physics and radiative transfer.

First, it is necessary to understand that the stellar spectrum is formed only in the surface layers of a star, called the *stellar photosphere*, although in cool stars the chromosphere and the corona also contribute to the emergent spectrum, especially in the far and extreme ultraviolet. The stellar photosphere plays such an important role in the formation of the spectrum because it is here that photons undergo their last few, and thus most critical, interactions with matter before escaping to free space.

Energy in the form of photons, produced in the core of the star by nuclear reactions, reaches the surface of the star only after countless interactions with the material in the interior of the star. The interior of a star is composed of a nearly completely ionized plasma (a gas consisting of electrons and ions). This plasma interacts with the radiation field in the interior through the physical processes of electron scattering and free–free and bound–free (photoionization) absorption and emission by ions. Free–free absorption occurs when a free electron becomes able to absorb a photon when in the vicinity of an ion. Thus a gamma-ray photon produced in the core of the star random walks its way to the surface and, in the process, is degraded into hundreds of lower energy photons (mostly in the UV, optical, and infrared parts of the spectrum). In the interior, because of the high densities, the *mean free path* between interactions is very short—on the order of a centimeter in main-sequence stars. The high densities also mean that in the interior, collisions are extremely effective in coupling the radiation field with the thermal state of the gas. In this condition, the interior is very nearly in a perfect state of thermodynamic equilibrium, and, as a consequence, the material in the interior of the star radiates at the local temperature as a *blackbody radiator*. As we move toward the surface and encounter lower densities, the mean free path of a typical photon becomes much longer. In the stellar photosphere, the mean free path may measure in the kilometers; eventually a level in the stellar photosphere is reached at which it is highly probable that the photon will escape without further interaction. Since at each interaction the energy (wavelength) of the photon may be altered, it is clear that the last few interactions are most important in the formation of the emergent spectrum.

Because the mean free path of a typical photon in the stellar photosphere is quite long, this means that the radiation field is not so tightly coupled to the

local thermal state of the gas, and thus the assumption that the gas is in a state of thermodynamic equilibrium is no longer strictly valid. However, in high-density, high-pressure atmospheres (main-sequence stars), and to a more limited extent in giant and supergiant stars, *local thermodynamic equilibrium*, i.e., the assumption that each layer in the stellar photosphere is characterized thermodynamically and radiatively by the local gas temperature, is an acceptable approximation, at least for the discussion below.

The physical processes of electron scattering and free–free and bound–free absorption by ions are referred to collectively as sources of *continuous opacity*, as these processes can scatter or absorb and emit photons over a wide range of wavelengths. In the stellar atmosphere other forms of opacity come into play. In particular, bound–bound absorption (i.e., absorption in spectral lines, or *line opacity*) is important. As a consequence, opacity in the stellar photosphere is a strong function of wavelength; in the core of a spectral line the opacity is considerably higher than in the surrounding continuum, where the opacity is due only to continuum processes.

There is a temperature gradient in a stellar photosphere; neglecting the possible existence of extended outer layers of the atmosphere—e.g., the corona and the chromosphere—the top (outer layer) of the photosphere is considerably cooler than the "bottom" (inner layer). This temperature gradient is one of the most important factors in the formation of absorption lines in the stellar spectrum. To understand how an absorption line is formed, compare a continuum region of a stellar spectrum with a spectral line. In the continuum region the total opacity is relatively low, as only continuum processes contribute. This means that we can see at those wavelengths deeply into the photosphere to relatively hot layers and thus the emerging radiation flux is high. In the core of a spectral line the opacity is high, and thus the majority of the photons emerge from higher, cooler layers. This leads to a lower radiation flux in the core of the spectral line than in the surrounding continuum, and thus the formation of an absorption line (see Figure 2.11).

The core of an absorption line is therefore formed in the cool upper layers of the stellar photosphere, the surrounding continuum is formed at depth, and the wings of the absorption line in intermediate layers. This implies that if the continuous opacity is relatively high, the spectral line will be formed only over a limited range in the atmosphere, and thus will be weaker than if the continuous opacity were low. This suggests that the strength of a spectral line is in inverse proportion to the continuous opacity and in direct proportion to the line opacity. Factors that contribute to the line opacity include the abundance of the relevant element in the photosphere, the proportion of the atoms that are in the ionization state and the excitation state required for absorption in the spectral line under consideration, and the transition probability associated with the spectral line. If we let κ_λ represent the continuous opacity per unit mass at the wavelength of the spectral line, and l_λ the line opacity, we then have, to a first approximation,

$$\text{Line Strength} \propto \frac{l_\lambda}{\kappa_\lambda}. \tag{2.4.1}$$